Stability and cap formation mechanism of single-walled carbon nanotubes

D.-H. Oh* and Young Hee Lee†
Department of Physics and Semiconductor Physics Research Center, Jeonbuk National University, Jeonju 561-756, Korea
(Received 24 March 1998)

We use tight-binding total-energy calculations to investigate the energetics and the cap formation mechanism of single-walled carbon nanotubes. The present calculations of the edge energy and strain energy suggest the growth of armchair nanotubes to be energetically more favorable than the growth of zigzag nanotubes. The cap formation at the edge of both nanotubes is animated by the tight-binding molecular-dynamics simulations. The cap formation is immediately followed by the pentagon formation at the edge of both tubes. The role of transitions metals is further discussed. [S0163-1829(98)04835-8]

I. INTRODUCTION

Unlike other covalent materials, the carbon system has unique topological diversities. Diamond is known to be the most stable phase with strong covalent sp^3 hybridization with its counterpart the planar graphite phase (sp^2 hybridization). Since the advent of fullerene (cage) structures[1] and successful preparations of their massive quantities[2] in which its bonding nature is a mixture of sp^2 and sp^3 hybridizations, research has focused on the physical properties of fullerenes and its applications to many different fields. The unusual structural stability, the topological diversity, and high electronegativity leading to the doping controllability and superconductivity are characteristics of fullerenes, although the application of these materials in various fields is still challenging. Multiwalled tubular forms of a few hundred nanometers in diameter have also been found as a by-product of the fullerene formations.[3] Recent theoretical studies show that the multiwalled nanotubes can be grown via the edge interactions (called ''lip-lip'' interactions) mediated by strongly covalent adatoms between the tube walls.[4,5]

Single-walled nanotubes (SWNT's) have been synthesized with an additional small amount of transition metals during the carbon arc discharge or laser evaporization of graphite rod.[6–8,10] The SWNT reveals many unusual physical properties depending on the diameter and chirality. The armchair tubes (n,n) (Ref. 9) show a metallic behavior, whereas the zigzag tubes $(n,0)$ are semiconducting, except the tube chirality of $n=3k$, where k is an integer, which becomes metallic again.

The most abundant species among fullerenes is C_{60} with a diameter of 7.1 Å. The counterpart of fullerenes in the SWnT's is armchair (10,10) nanotubes with a diameter of 14 Å.[6,10] Strong electron field emission has been realized with carbon nanotubes[11] and further applied to field-emitting flat panel displays[12] and scanning tunnel microscope tips.[13] The small size of the diameter and controllability of the energy gap show potential application to high-density memory devices.

In spite of these applications, the reproducibility and controllability of the chirality and diameter have still not been achieved experimentally. In particular, a small amount of transition metals gives very high yields of SWNT's and most of the cage structures are not reproduced. The long tubes, as long as about 0.1 mm, have been turned out to be mostly armchair tubes,[6,10] although the early observations show some other chiral nanotubes.[14] However, the role of transition metals is not clearly known. It has been proposed that the transition metal adsorbs strongly at the edge, but the diffusion barrier is low (~ 1 eV) enough that the Ni atom can migrate along the edge of the tube easily like a scooter motion, thus efficiently catalyzing the topological defects such as pentagons and heptagons.[15]

In this study we describe the detailed energetics of the tube edges and cap formation mechanism using *ab initio* calculations based on the local-density approximation (LDA) and tight-binding molecular-dynamics (TBMD) simulation techniques. The cap formation procedure is vividly visualized through animation.

II. THEORETICAL APPROACHES

Our calculations have been carried out using the TBMD method. We introduce an efficient semiempirical tight-binding (TB) approach for large-scale calculations such as the cap formation process of carbon nanotubes. In the TB approach of carbon system, the band structure energy is parametrized using the Slater-Koster scheme[16] with an orthogonal sp^3 basis set in which the positional dependence is scaled by an extra exponential factor.[17] The repulsive ion-ion potentials are fitted similarly to the band structure energy. This reproduces the qualitative behaviors of the total-binding-energy curves of various phases obtained from the LDA calculations[17] and has been successfully applied to fullerene systems.[18] The conjugate-gradient (CG) approach is applied to get the ground-state equilibrium structures. We also employ the TBMD method in order to study the dynamical behavior of tubes.

III. RESULTS AND DISCUSSION

The coexistence of stable diamond and graphite provides more complex topological varieties in the geometry. Compared to the graphitic layered structures, cage structures (fullerenes) and tubes require excessive strain energy. Figure 1 shows the relative stain energies of each structure with respect to the graphitic layer. We take 180 carbon atoms in the form of a graphitic layer with two-dimensional periodic boundary conditions and calculate the total energy by the TB total-energy method. The C-C distance is taken to be 1.42 Å. The total energy of the C_{60} cage structure is calculated by the CG relaxation scheme in which three times this total energy

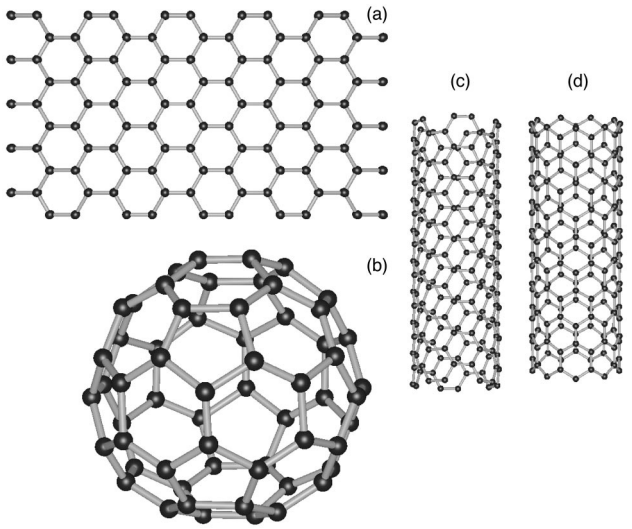

FIG. 1. Carbon architecture: (a) graphitic layer, (b) fullerence C_{60}, (c) armchair (5,5) nanotube, and (d) zigzag (9,0) nanotube. The relative strain energies of structures (b)–(d) with respect to (a) the graphitic layer are 0.352, 0.355, and 0.395 eV/atom.

is compared to that of the graphitic layer. Two characteristic bond lengths of 1.39 and 1.45 Å in C_{60} are obtained. The heavy strain energy of 0.352 eV/atom is contributed from the pentagon formation and the spherical curvature of C_{60}. In spite of quite a large amount of strain involved in C_{60}, cage structures are found in nature, suggesting that local metastable structures and/or high-temperature nonequilibrium dynamics are important. For nanotubes where the periodic boundary condition is applied to the tube axis only, we can form two achiral tubes depending on the wrapping direction. Each structure is fully optimized by the CG method. The armchair (5,5) tube in which the diameter (6.9 Å) is similar to that of C_{60} gives a similar strain energy to C_{60}, whereas the zigzag (9,0) tube whose diameter (7.0 Å) is again similar to that of C_{60} gives larger strain energy by 0.04 eV/atom than the armchair tube. This suggests that the armchair tube might be formed more easily than the zigzag tube.

It is not clear whether or not the armchair tubes are more favorable than the zigzag tubes. Recent experimental observations[6,10] mostly show the armchair tubes, although some previous observations show the zigzag and even chiral tubes.[14] Perhaps one of the interesting quantities in determining the relative stability of the tubes is the edge energy. We calculate the edge energy of each tube by defining the energy with respect to the graphitic layer

$$\Delta E^{(5,5)} = E^{(5,5)}_{total} - E^{graphite}_{total}, \quad \Delta E^{(9,0)} = E^{(9,0)}_{total} - E^{graphite}_{total}. \tag{1}$$

Similarly to the previous calculations, we take 180 carbon atoms for each calculation. We leave the edges of the tubes open in this case. Each edge structure is again optimized by the TB-CG method. The armchair edge is stabilized by forming a strong covalent bond with a bond length of 1.28 Å [1.23 Å from the LDA,[15] comparable to the triple bond (1.2 Å) of C_2H_2], whereas the zigzag edge forms an intermediate bond (1.44 Å) between single and double bonds (1.40 and 1.46 Å in C_{60}). The corresponding bond lengths are shown in

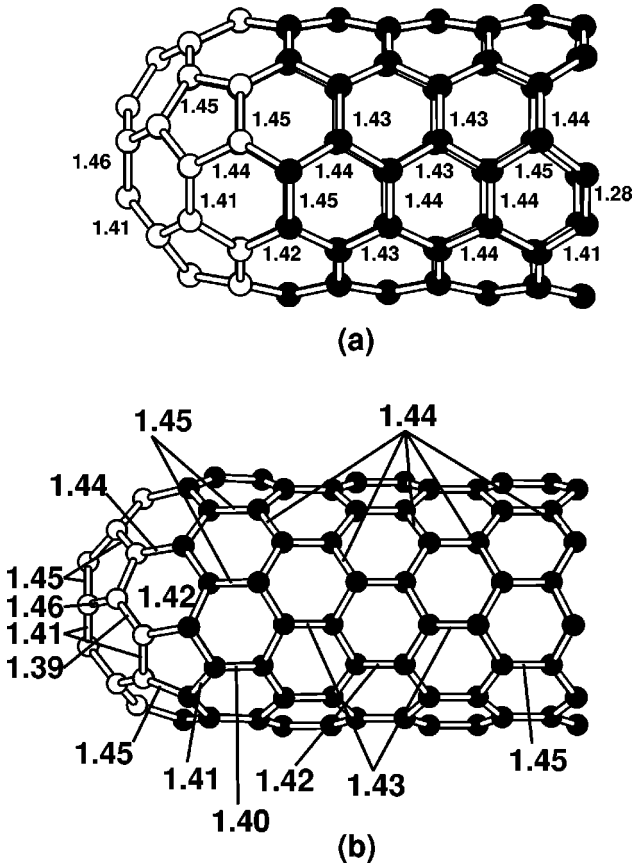

FIG. 2. Fully relaxed capped nanotubes with an open end: (a) armchair tube and (b) zizag tube. The open circles indicate the cap atoms. All lengths are in angstroms.

Fig. 2. By dividing the edge energy by the number of atoms at the open edge, we get $\Delta E^{(5,5)} = 3.19$ eV/atom and $\Delta E^{(9,0)} = 3.95$ eV/atom. Thus the armchair tube edge is more stable by 0.76 eV/atom than the zigzag tube edge, which is comparable to 0.79 eV/atom from the LDA calculations.[15]

Another interesting quantity is the energy gain by the cap formation energy. The tube usually terminates with a dome closure. The local topology of the cap formation for the armchair and zigzag tubes is different, as shown in Fig. 2. The cap of the armchair tube is obtained by selecting a hemisphere of C_{60} that possesses a pentagon pole at the top of the center, while the cap of the zigzag tube is obtained by selecting a hemisphere of C_{60} that possesses a hexagon pole at the top of the center. The armchair cap has ten edge atoms, whereas the zigzag cap has nine edge atoms. We first relax individual caps and the tube with open edges by the TB-CG method. The energy gain by the cap formation can be obtained by subtracting the total energies of the respective cap and tube from the total energy of the combined cap and tube. The energy gain of the armchair tube due to cap formation is -40.1 eV $= -0.4$ eV/edge atom, whereas the energy gain of the zigzag tube due to cap formation is -70.5 eV $= -7.8$ eV/edge atom. This significant energy gain is due to the stable edge formed with covalent triple bonds at the armchair tube edge and the singly coordinated atoms at the edge of the zigzag tube. Even in the case of the zigzag cap with 21 atoms such that the edge atoms of both the cap and zigzag

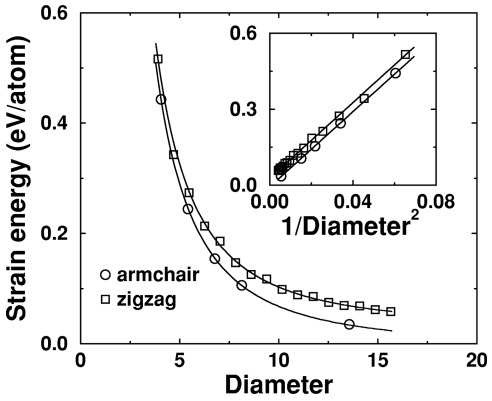

FIG. 3. Strain energy per carbon atom of armchair and zigzag nanotubes with respect to the total energy of the graphitic layer as a function of tube diameter. The inset shows clearly the strain energy depending on the inverse square of the diameter. The diameter is in angstroms.

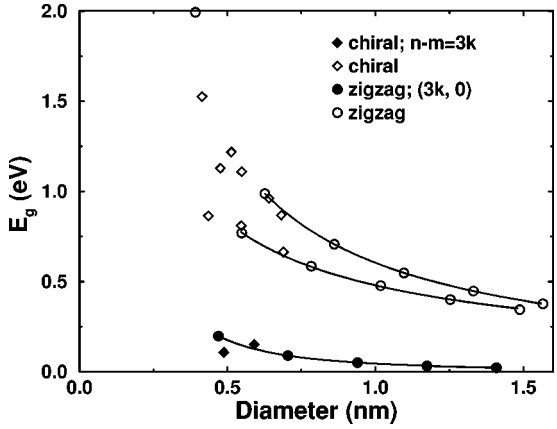

FIG. 4. Energy gap as a function of diameter for different chiral tubes. The filled circles indicate the bend-induced gap of zigzag $(n,0)$ tubes with $n=3k$. The filled diamonds are also the bend-induced gap of chiral (n,m) tubes with $n-m=3k$. Open circles indicate the energy gap of the zigzag $(n,0)$ with $n-m\neq 3k$, resulting from the rehybridization of π-π^* orbitals. The energy gap of chiral tubes falls into the region of the energy gap of zigzag tubes.

tube are doubly coordinated [open atoms in Fig. 2(b)], the zigzag tube still gains an energy of -0.44 eV/edge atom over the armchair tube. It is also interesting to compare the energy gain of C_{60} combined with two caps with that of the combined armchair and cap. The energy gain of the combined two C_{30} caps to form C_{60} is -42.4 eV, 2.3 eV more stable than that of the latter case. From the evaluation of the energy gain due to the cap formation, it can be suggested that C_{60} is more easily formed than any type of tube and furthermore the armchair tube has a better chance than the zigzag tube to survive for long tube growth without a dome closure.

We also study the relative stability of the armchair and zigzag tubes. Figure 3 shows the strain energies as a function of diameter where the strain energy of each tube is calculated from the total energy difference with respect to the graphitic layer. The periodic boundary condition along the tube axis is applied in the tube calculations. The strain energy of the zigzag tube is always larger than that of the armchair tube over all range of diameters. For instance, the (5,5) armchair tube has a smaller strain energy by 0.04 eV/atom than its counterpart of the (9,0) zigzag tube. The nearest-neighbor distance along the circumference of the armchair tube is 1.42 Å, whereas this is 2.46 Å in the zigzag tube. The short distance of the armchair tube makes the stronger rehybridization of π orbitals during wrapping of the graphitic sheet. The inset clearly shows that both tubes follow the classical elasticity theory, where the strain energy is inversely proportional to the square of the diameter. This suggests again that the armchair tube is more easily formed than the zigzag tube. From the above calculations of the relative stability, edge energy, and strain energy, we note that the zigzag tube is energetically unfavorable to the armchair tube in the formation process.

We now calculate the energy gaps as a function of diameter and will show that the energy gap also depends seriously on the diameter particularly for tubes with a small diameter. From the symmetry of the Brillouin zone of the graphitic layer,[19] the armchair tube (n,n) is always metallic due to the crossing of π-π^* at the K point, although the elastic energy opens the gap and is not negligible, particularly for smaller diameters[20] where the contribution of the strain (bending) energy becomes significant. For the zigzag tube $(n,0)$, when the chirality is $(3k,0)$, where k in an integer, the accidental symmetric point in the Brillouin zone overlaps at the Γ point, giving again no energy gap. For all tubes (n,m) in which $n\neq m$ and $n-m\neq 3k$, the finite size of the energy gap exists. Figure 4 shows the energy gaps as a function of diameter for different chiralities. It reveals two major categories of the gap. The primary gap with filled circles in the case of $(3k,0)$ tubes is not zero but finite and approaches a zero gap with increasing diameter. The energy gap of the armchair tube is not shown but always a zero gap due to the crossing of π-π^* orbitals. The finite gap results from the bending energy, which simply almost fits d^{-2}. The chiral tube (n,m) with $n-m=3k$ shows behavior similar to the zigzag tube $(3k,0)$. The secondary gap of zigzag tubes shows two slopes. When $n=3k+1$, the energy gap is proportional to $d^{-0.79}$ and when $n=3k+2$ it is proportional to $d^{-1.05}$. Both are close to d^{-1} and the major contribution to this behavior is the rehybridization of the π orbitals due to the finite curvature of the tube. It should be noted that this small energy gap due to the nonzero curvature even in the case of metallic armchair tubes and zigzag tubes with zero gap will have important consequences for low-temperature quantum transport properties.[21,22]

Although a considerable amount of energy is gained by the cap formation process, the growth process in an atomic scale is still far from being clearly understood. Here we perform the TBMD simulational approaches to see how the carbon atoms adsorb on the tube edge to either grow further or come to a dome closure. We start with the capped tube at the bottom and open edge at the top of the tube. Initially we add the number of carbon atoms for each tube (30 for the armchair and 29 for the zigzag) in a gas phase. The gaseous carbon atoms are constrained to stay within a sphere with a diameter of 14 Å centered at the tube axis separated by about 7 Å from the top edge of the tube as shown in Fig. 5(a). We use 130 and 157 carbon atoms for armchair and zigzag tubes, respectively. The initial temperature was set to 2000 K. The time step is 1.12×10^{-16} s. The velocities are rescaled to give the desired temperature. The first few hundred steps are

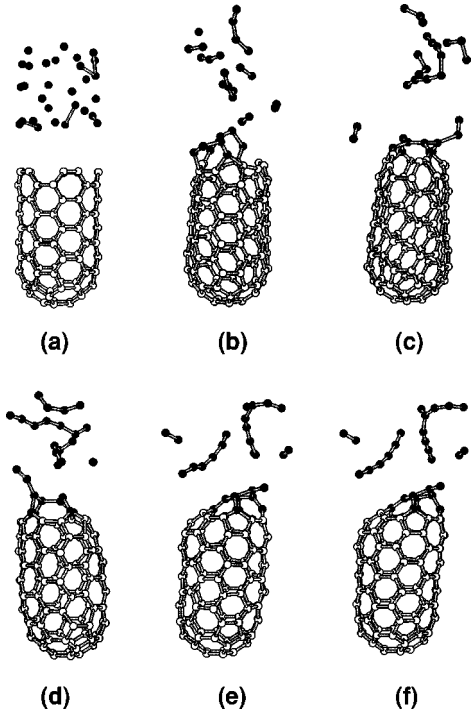

FIG. 5. Typical snapshot (side view) of gaseous carbon adsorption on an armchair tube edge using the TBMD simulation at $T = 2000$ K for different simulation times: (a) initial snapshot after equilibrium, (b) $t = 1.12$ ps, (c) 1.96 ps, (d) 2.52 ps, (e) 5.6 ps, and (f) optimized structure by the CG relaxation from the final geometry at 5.6 ps. Adatoms are drawn with filled circles and atoms at the tube are drawn with open circles. The bonds are drawn when the distance is within 1.9 Å.

run to equilibrate the system. The total simulation time for canonical run was 5.6 ps. Figure 5 shows several snapshots of the time evolution of the cap formation process for the armchair tube. Some gaseous carbon atoms form a dimer and trimer initially as shown in Fig. 5(a). Adatoms approach the edge of the tube and have a chance to form a pentagon as shown in Fig. 5(b). Since the temperature is not very high, the adatom forming a pentagon would not diffuse to other sites. Once a pentagon is formed, this induces the tube edge to close to the inner direction. Further adsorption of carbon atoms join them to form a dome closure, while some gaseous atoms are now linearized, still with dimers and trimers. It is also easy to observe the heptagon formation as shown in Figs. 5(d)–5(e). Once a heptagon is formed, a negative curvature is developed, which is often observed as bending tubes. In addition, gaseous adatoms are further linearized. One can see a combination of pentagon and heptagon clearly after the CG relaxation to zero temperature from Fig. 5(f). Chains are more completely linearized due to the removal of entropy effects.

Figure 6 shows similar snapshots for zigzag tubes. The gaseous carbon atoms approach the edge of the zigzag tubes with a preferable form of linear chains that bond to the top site of the tube edge, as shown in Fig. 6(b). These linear chains connected to adjacent top sites intervene with each other [Fig. 6(c)] and have a chance to form a pentagon, which appears in Fig. 6(d). Again, once a pentagon is formed, a dome closure follows immediately. In this case a dome closure process is accelerated more completely due to

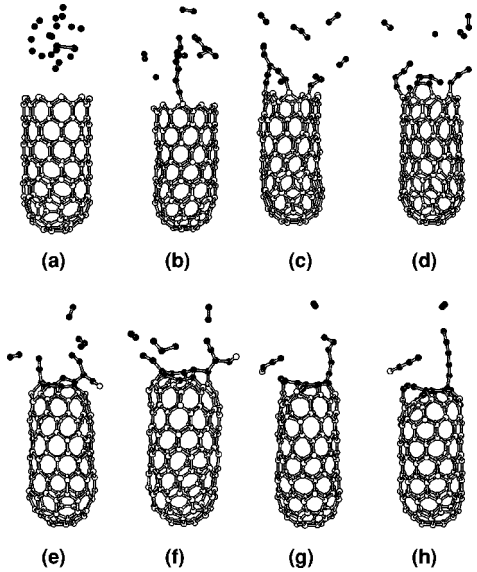

FIG. 6. Typical snapshot (side view) of gaseous carbon adsorption on a zigzag tube edge using the TBMD simulation at $T = 2000$ K for different simulation times: (a) initial snapshot after equilibrium, (b) $t = 0.84$ ps, (c) 1.96 ps, (d) 2.52 ps, (e) 3.64 ps, (f) 4.2 ps, and (g) optimized structure by the CG relaxation from the final geometry obtained at 5.6 ps. Adatoms are drawn with filled circles and atoms at the tube are drawn with open circles. The bonds are drawn when the distance is within 1.9 Å.

the coexistence of pentagons at adjacent sites. We also note that one atom from the tube edge desorbs and forms a bond with a chain in the vacuum. This suggests that the edge of the zigzag tubes is less stable than that of the armchair tubes, reflecting the stable edge formation of the armchair tubes, as demonstrated in previous calculations of the edge energy.

It will be very intuitive to illustrate a honeybee's eye for pedagogical purpose in relation to the cap formation. Figure 7 shows the flat part and corner of the honeybee's eye. The

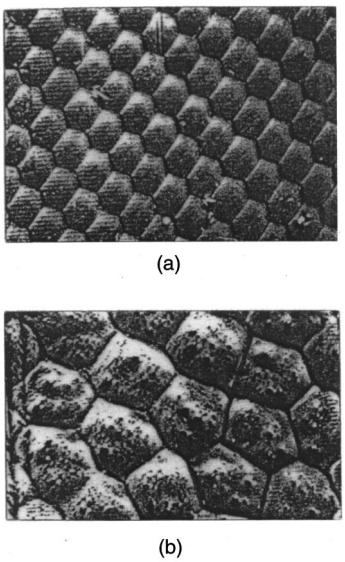

FIG. 7. (a) Complete hexagon pattern in the noncurved part of the honeybee's eye and (b) defect pattern with pentagons in the corner of the honeybee's eye. Photos taken at Daresbury Laboratory, Daresbury, Warrington, Cheshire, England.

noncurved part forms complete hexagons, whereas the corner of the honeybee's eye is curved and thus the hexagon is no longer stable but the strain energy is minimized by forming pentagons. Note that no heptagon that leads to negative curvature is formed. This is in analogy with the cap formation process of the tube. Whenever pentagons are formed at the edge of the tube, there is a tendency to have a dome closure unless they are annealed away in some other way. This will be discussed in the next paragraph.

In armchair tubes, a single adatom forms a pentagon at the seat site and becomes a seed for cap formation. A single adatom at the arm site is another locally stable site and will either have a chance to diffuse to the next site or stay until a new adatom approaches. On the other hand, a dimer at the seat site is a complete unit that forms a hexagon at the edge. In the zigzag tube, a dimer is a unit for pentagon formation, leading to a dome closure. A single adatom on top and bridge sites is locally stable and may more easily diffuse to the next site than the arm site on the armchair tube. A trimer is a complete unit in zigzag tubes. In the case of linear chains approaching the edge of both tubes, any type of defect can be created. These defects will eventually lead to a dome closure, unless these defects are annealed away in some other way. A high growth temperature usually helps to anneal away these defects, but again a too high temperature will either evaporate adatoms easily to the atmosphere or destroy the tube formation. Another way is to introduce a small amount of transition metals in the system as experimentally observed.[6,10,14,23–25] Fast Ni motion at the edge of the tube was proposed recently.[15,26] This fast scooting motion enables one to anneal away efficiently the defect formation at the edge of armchair tube.

IV. SUMMARY

We have evaluated various energetics of armchair and zigzag nanotubes using tight-binding total-energy calculations. The edge energy shows the armchair tube to be energetically more favorable than the zigzag tube. Both the armchair and zigzag nanotubes follow the classical elastic theory with increasing diameter size. More strain energy is required to form zigzag tubes than armchair nanotubes over the whole region of the diameter. The energy gap is also evaluated as a function of diameter including chiral tubes. Two major gaps exist. The band gap of the zigzag and chiral tubes also follow the trend of strain energy. In the TBMD simulation, we observe that whenever a pentagon is formed at armchair and zigzag tubes, the tubes will eventually lead to a dome closure, terminating tube growth.

ACKNOWLEDGMENTS

We acknowledge financial support by the Korea Research Foundation made in the program year of 1997 and the Korea Science and Engineering Foundation (KOSEF) through the Semiconductor Physics Research Center at Jeonbuk National University.

*Present address: Center for Biofunctional Molecules, Pohang University of Science and Technology, Pohang 790-784, Korea.

†Author to whom correspondence should be addressed. Electronic address: leeyh@sprc2.chonbuk.ac.kr

[1] H. W. Kroto, J. R. Heath, S. C. O'Brien, R. F. Carl, and R. E. Smalley, Nature (London) **318**, 162 (1985).

[2] W. Krätschmer, L. D. Lamb, K. Kostiropoulos, and D. R. Huffman, Nature (London) **352**, 480 (1991).

[3] S. Iijima, Nature (London) **354**, 56 (1991).

[4] Y. K. Kwon, Y. H. Lee, S. G. Kim, P. Jund, D. Tománek, and R. E. Smalley, Phys. Rev. Lett. **79**, 2065 (1997).

[5] J.-C. Charlier, A. De Vita, X. Blase, and R. Car, Science **275**, 646 (1997).

[6] A. Thess, R. Lee, P. Nikolaev, H. Dai, P. Petit, J. Robert, C. Xu, Y. H. Lee, S. G. Kim, D. T. Colbert, G. Scuseria, D. Tománek, J. E. Fisher, and R. E. Smalley, Science **273**, 483 (1996).

[7] T. Guo, P. Nikolaev, A. Thess, D. T. Colbert, and R. E. Smalley, Chem. Phys. Lett. **243**, 49 (1995).

[8] S. Witanachchi and P. Mukherjee, J. Vac. Sci. Technol. A **13**, 1171 (1995).

[9] M. S. Dresselhaus, G. Dresselhaus, and P. C. Eklund, *Science of Fullerenes and Carbon Nanotubes* (Academic, San Diego, 1996), Chap. 19, and references therein.

[10] M. Terrones, N. Grobert, J. Olivares, J. P. Zhang, H. Terrones, K. Kordatos, W. K. Hsu, J. P. Hare, P. D. Townsend, K. Prassides, A. K. Cheetham, H. W. Kroto, and D. R. M. Walton, Nature (London) **388**, 52 (1997).

[11] A. G. Rinzler, J. H. Hafner, P. Nikolaev, L. Lou, S. G. Kim, D. Tománek, P. Nordlander, D. T. Colbert, and R. E. Smalley, Science **269**, 1550 (1995).

[12] W. A. de Heer, A. Chatelain, and D. Ugarte, Science **270**, 1179 (1995).

[13] H. Dai, J. H. Hafner, A. G. Rinzler, D. T. Colbert, and R. E. Smalley, Nature (London) **384**, 147 (1996).

[14] S. Iijima and T. Ichihashi, Nature (London) **363**, 603 (1993).

[15] Y. H. Lee, S. G. Kim, and D. Tománek, Phys. Rev. Lett. **78**, 2393 (1997).

[16] J. C. Slater and G. F. Koster, Phys. Rev. **94**, 1498 (1954).

[17] C. Z. Wang, C. H. Xu, C. T. Chan, and K. M. Ho, J. Phys.: Condens. Matter **4**, 6047 (1992).

[18] E. Kim, Y. H. Lee, and J. Y. Lee, Phys. Rev. B **48**, 18 230 (1993).

[19] N. Hamada, S. Sawada, and A. Oshiyama, Phys. Rev. Lett. **68**, 1579 (1992).

[20] C. L. Kane and E. J. Mele, Phys. Rev. Lett. **78**, 1932 (1997).

[21] J. E. Fischer, H. Dai, A. Thess, R. Lee, N. M. Hanjani, D. L. Dehaas, and R. E. Smalley, Phys. Rev. B **55**, 4921 (1997).

[22] P. Delaney, H. J. Choi, J. Ihm, S. G. Louie, and M. L. Cohen, Nature (London) **391**, 466 (1998).

[23] D. S. Bethune, C. H. Kiang, M. S. deVries, G. Gorman, R. Savoy, J. Vazquez, and R. Beyers, Nature (London) **363**, 605 (1993).

[24] P. M. Ajayan, J. M. Lambert, P. Bernier, L. Barbedette, C. Colliex, and J. M. Planeix, Chem. Phys. Lett. **215**, 509 (1993).

[25] J. M. Lambert, P. M. Ajayan, P. Bernier, J. M. Planeix, V. Brotons, B. Coq, and J. Castaing, Chem. Phys. Lett. **226**, 364 (1994).

[26] Y. H. Lee, J. Korean Phys. Soc. **31**, s263 (1997).